Available online at www.sciencedirect.com
SCIENCE DIRECT®
Physics of the Earth and Planetary Interiors 151 (2005) 89–106
PHYSICS OF THE EARTH AND PLANETARY INTERIORS
www.elsevier.com/locate/pepi

Earth gravity up to second order in topography and density

Frédéric Chambat[a,*], Bernard Valette[b]

[a] Laboratoire de Sciences de la Terre, ENS-Lyon, 46 Allée d'Italie, 69364 Lyon Cedex 07, France
[b] LGIT, IRD, Université de Savoie, 73376 Le Bourget-du-Lac Cedex, France

Received 28 June 2004; received in revised form 22 December 2004; accepted 26 January 2005

Abstract

The gravity potential of a planet is usually expanded up to first order only as a linear function of topography and lateral variations of density. In this article, we extend these expressions up to second order and we estimate the magnitude of the new non-linear terms. We find that they are not negligible when compared to observed values: tens of metres for height anomalies and tens of milligals for gravity anomalies. Therefore, second-order expressions should be taken into account when inverting global gravity data.

Keywords: Gravity; Potential; Density; Topography; Perturbation

1. Introduction

In order to interpret the observed gravity potential anomalies of planets, the potential is usually expressed as a linear function of the lateral variations of density and topography. These relations are first-order approximations in the vicinity of a spherical reference. It has long been observed that the Earth gravity anomalies are much less than those due to the external topography only; this is the consequence of the isostatic compensation, which results in a quasi-cancellation of the external topography contribution with that of the Moho.

As the sum of the terms involved in the first-order gravity potential nearly cancel, we may wonder what the magnitude of the second-order terms is. The aim of this article is to answer this question. First, we give the expression of the potential complete to the second order in topography and lateral density variations (Sections 2–4). Second, we give a numerical estimation of the second-order terms and compare their magnitude with the observed gravity and potential (Section 5).

Non-linear evaluations of the potential have already been considered: Balmino (1994) has given the expression of the potential of an homogeneous body up to second order in its topography and has applied it to Phobos. Martinec (1994) has used similar expressions and a crustal topographic model to estimate the density jump at the Moho by minimizing the external potential. Numerical methods were used to accurately calculate

* Corresponding author. Tel.: +33 47 2728556; fax: +33 47 2728677.
E-mail addresses: Frederic.Chambat@ens-lyon.fr (F. Chambat), Bernard.Valette@univ-savoie.fr (B. Valette)

0031-9201/$ – see front matter © 2005 Elsevier B.V. All rights reserved.
doi:10.1016/j.pepi.2005.01.002

the potential of models given on a spatial grid: Ilk et al. (1996) have proposed an algorithm based on a division of the model in spherical cells, Kaban et al. (1999) have computed the potential of an isostatic lithosphere, and Belleguic (2004) have computed Mars gravity field. However, none of them has given the general expression for the second-order potential, or has made any comparison with the observed values for the Earth. In particular, the coupling of the hydrostatic shape with non-hydrostatic structures has not been evaluated. High-order calculations of the gravitational potential have been performed in planar geometry by Oldenburg (1974) with a method due to Parker and Huestis (1974), and by Ockendon and Turcotte (1977).

In geodesy, similar calculations have been performed to precisely estimate the geoid from the external potential, which only involves the masses that lie outside the geoid. For example, Sjöberg (1995, 1998a,b), Nahavandchi and Sjöberg (1998), and Rapp (1997) have pointed out the importance of the second and third order in topography. But basically, the problem in geophysics is to fit the external potential with an internal mass model and not, as in geodesy, to precisely determine the shape of the geoid.

In a previous work, we have estimated the perturbations of Earth's mass and inertia (Chambat and Valette, 2001). The present article can be considered as its complement to higher harmonic degree coefficients of the potential. We use the same notations: b is the mean radius of the Earth, G the gravitational constant, ρ the density field, and r, θ, λ are the spherical coordinates (radius, colatitude, longitude).

2. Expression of the gravitational potential

Outside a planet, the gravitational potential φ is harmonic and can be written

$$\varphi(r,\theta,\lambda) = \sum_{\ell=0}^{\infty}\sum_{m=-\ell}^{\ell}\left(\frac{b}{r}\right)^{\ell+1}\varphi_\ell^m(b)Y_\ell^m(\theta,\lambda). \tag{1}$$

The Y_ℓ^m are the spherical harmonics defined in Appendix A and the coefficients $\varphi_\ell^m(b)$ depend on the density as

$$\varphi_\ell^m(b) = -\frac{G}{(2\ell+1)b^{\ell+1}}\int_V \rho(r,\theta,\lambda)r^\ell Y_\ell^m(\theta,\lambda)\,\mathrm{d}V, \tag{2}$$

where V is the Earth's volume. Note that our sign convention is such that the gravity vector is $-\mathrm{grad}\,\varphi$. We denote by ϕ_ℓ^m the integral with which we will deal throughout the article:

$$\phi_\ell^m = \int_V \rho(r,\theta,\lambda)r^\ell Y_\ell^m(\theta,\lambda)\,\mathrm{d}V. \tag{3}$$

The low degree coefficients are easy to interpret: ϕ_0^0 is the Earth's mass $\mathcal{M}$, the ϕ_1^m are related to the position of the centre of mass, and the ϕ_2^m are related to the inertia tensor.

Most of the time, the integral in (3) is expressed to first order as a linear function of lateral perturbations of density and topography. Our purpose is to extend these expressions up to second order. Note that the potential is linear in density and that the non-linear terms arise from the non-spherical shape of the interfaces.

After having subtracted a reference potential, such that of a hydrostatic quasi-ellipsoid, two quantities are usually derived from φ. First, the height anomaly is defined by

$$\zeta(\theta,\lambda) = -\frac{\varphi(r=b,\theta,\lambda)}{g}, \tag{4}$$

where g is the norm of the reference gravity at the surface:

$$g = \frac{G\mathcal{M}}{b^2} = \frac{4}{3}\pi G\rho_2 b, \tag{5}$$

and ρ_2 is the mean density. Correct to first order, ζ represents the height of the equipotential, i.e. the geoid undulation, above the surface of reference. Second, the gravity anomaly is defined by

$$\delta g(\theta,\lambda) = \left(\frac{\partial}{\partial r}+\frac{2}{r}\right)\varphi(r=b,\theta,\lambda), \tag{6}$$

which, correct to first order, is the free air anomaly. Although these interpretations are correct to first order only, ζ and δg constitute an easy and classical way to represent φ (Heiskanen and Moritz, 1967; Sjöberg, 1995; Rapp, 1997). The spherical harmonic decompositions of these relations lead to

$$\zeta_\ell^m = -\frac{\varphi_\ell^m(b)}{g}, \qquad \frac{\delta g_\ell^m}{g} = (\ell-1)\frac{\zeta_\ell^m}{b}. \tag{7}$$

Owing to coefficient $\ell-1$ in Eq. (7) defining δg_ℓ^m, maps of gravity anomalies provide finer details than maps of height anomalies do.

We can rewrite relations (7) as functions of ϕ_ℓ^m (3) and ρ_2 (5):

$$\zeta_\ell^m = \frac{\phi_\ell^m}{(2\ell+1)b^{\ell-1}\mathcal{M}} = \frac{3\phi_\ell^m}{4\pi(2\ell+1)b^{\ell+2}\rho_2}, \tag{8}$$

$$\frac{\delta g_\ell^m}{g} = \frac{(\ell-1)\phi_\ell^m}{(2\ell+1)b^{\ell}\mathcal{M}} = \frac{3(\ell-1)\phi_\ell^m}{4\pi(2\ell+1)b^{\ell+3}\rho_2}. \tag{9}$$

It yields

$$\frac{\phi_\ell^m}{b^\ell} = \mathcal{M}\left(2\frac{\delta g_\ell^m}{g} + 3\frac{\zeta_\ell^m}{b}\right) = \frac{4}{3}\pi\rho_2 b^3\left(2\frac{\delta g_\ell^m}{g} + 3\frac{\zeta_\ell^m}{b}\right). \tag{10}$$

3. Shape perturbations

In order to evaluate ϕ_ℓ^m we make use of the shape perturbation formalism and the notations given in Chambat and Valette (2001). In this approach, the Earth is related to the reference model by a continuous deformation. Then the physical parameters of the Earth can be derived from those of the reference model through a Taylor expansion. This defines the perturbations to the different orders. In this section, we recall some notations and relations of this perturbation formalism.

3.1. Lagrangian and Eulerian perturbations

First, we define a mean model as in Chambat and Valette (2001): we choose a continuous stratification of surfaces S extrapolating the interfaces Σ and we define the mean radius of a given surface by r. Each point $\boldsymbol{x}(r, \theta, \lambda)$ of S with density $\rho(\boldsymbol{x})$ in the Earth is then related to a point $\boldsymbol{a}(r, \theta, \lambda)$ with density $\rho_0(r)$ in the mean model (Fig. 1), this reference density being defined by angular averaging of $\rho(\boldsymbol{x})$.

Second, the virtual deformation of the Earth domain is parameterized by a scalar t ranging from 0, for the reference configuration, to 1, for the Earth. We thus consider the following mapping:

$$\forall(\boldsymbol{a}, t) \in V_0 \times [0,1] \to \boldsymbol{x}(\boldsymbol{a}, t) \in V_t, \tag{11}$$

with $\forall \boldsymbol{a} \in V_0, \boldsymbol{x}(\boldsymbol{a}, 0) = \boldsymbol{a},\ \boldsymbol{x}(\boldsymbol{a}, 1) = \boldsymbol{x}$ and $V_{t=0} = V_0,\ V_{t=1} = V$. For any regular tensor field $\boldsymbol{T}$, we can

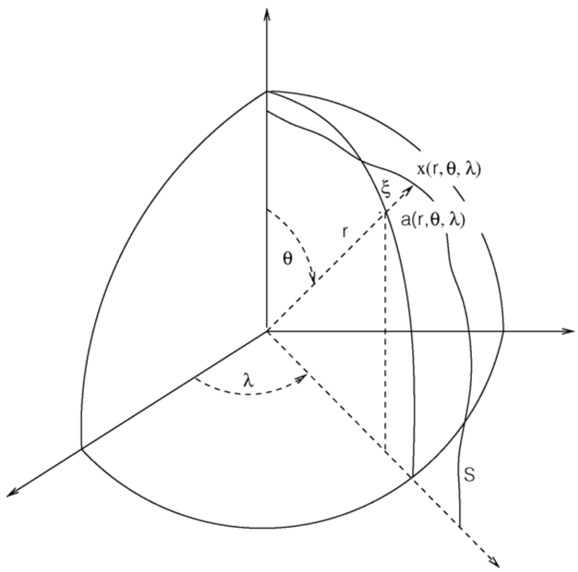

Fig. 1. Notations used to define the reference configuration. The surfaces S which extrapolate the Earth interfaces have mean radii r. The points $\boldsymbol{x}$ of S are referenced by the points $\boldsymbol{a}$ on the spheres of radii r. $\boldsymbol{\xi} = \boldsymbol{x} - \boldsymbol{a}$ is the radial Lagrangian vector between the two configurations. θ is the colatitude and λ the longitude.

consider the mapping $(\boldsymbol{a}, t) \to \boldsymbol{T}(\boldsymbol{x}(\boldsymbol{a}, t), t)$. The Lagrangian displacement of order n is defined by

$$\boldsymbol{\xi}_n(\boldsymbol{a}) = \left.\frac{\mathrm{d}^n}{\mathrm{d}t^n}\boldsymbol{x}(\boldsymbol{a}, t)\right|_{t=0}, \tag{12}$$

and the Eulerian, respectively, Lagrangian, perturbations of order n of $\boldsymbol{T}$ by

$$\delta_{ne}\boldsymbol{T}(\boldsymbol{a}) = \left.\frac{\partial^n}{\partial t^n}\boldsymbol{T}(\boldsymbol{x}(\boldsymbol{a}, t), t)\right|_{t=0}, \tag{13}$$

$$\delta_{nl}\boldsymbol{T}(\boldsymbol{a}) = \left.\frac{\mathrm{d}^n}{\mathrm{d}t^n}\boldsymbol{T}(\boldsymbol{x}(\boldsymbol{a}, t), t)\right|_{t=0}. \tag{14}$$

As a consequence:

$$\delta_{ne}\boldsymbol{x} = 0 \quad \text{and} \quad \delta_{nl}\boldsymbol{x} = \boldsymbol{\xi}_n. \tag{15}$$

Defining $\boldsymbol{\xi}$, $\delta_e\boldsymbol{T}$ and $\delta_1\boldsymbol{T}$, respectively, by

$$\boldsymbol{x}(\boldsymbol{a}, 1) = \boldsymbol{a} + \boldsymbol{\xi}(\boldsymbol{a}), \tag{16}$$

$$\boldsymbol{T}(\boldsymbol{a}, 1) = \boldsymbol{T}(\boldsymbol{a}, 0) + \delta_e\boldsymbol{T}(\boldsymbol{a}), \tag{17}$$

$$\boldsymbol{T}(\boldsymbol{x}(\boldsymbol{a}, 1), 1) = \boldsymbol{T}(\boldsymbol{a}, 0) + \delta_1\boldsymbol{T}(\boldsymbol{a}), \tag{18}$$

a Taylor expansion to order N yields

$$\boldsymbol{\xi}(\boldsymbol{a}) = \sum_{n=1}^{N} \frac{1}{n!} \boldsymbol{\xi}_n(\boldsymbol{a}), \tag{19}$$

$$\delta_e \boldsymbol{T}(\boldsymbol{a}) = \sum_{n=1}^{N} \frac{1}{n!} \delta_{ne} \boldsymbol{T}(\boldsymbol{a}), \tag{20}$$

$$\delta_l \boldsymbol{T}(\boldsymbol{a}) = \sum_{n=1}^{N} \frac{1}{n!} \delta_{nl} \boldsymbol{T}(\boldsymbol{a}). \tag{21}$$

3.2. First-order relations

Consider now a scalar field f and a vector field $\boldsymbol{u}$. It is easy to show that, to first order

$$\delta_{1l} f = \delta_{1e} f + \operatorname{grad} f \cdot \boldsymbol{\xi}_1, \tag{22}$$

$$\delta_{1l}(\operatorname{div} \boldsymbol{u}) = \operatorname{div}(\delta_{1l}\boldsymbol{u}) - \operatorname{tr}(\nabla\boldsymbol{u} \cdot \nabla\boldsymbol{\xi}_1), \tag{23}$$

$$\delta_{1l}(\operatorname{grad} f) = \operatorname{grad}(\delta_{1e} f) + \nabla\nabla(f)\boldsymbol{\xi}_1, \tag{24}$$

where the second-order tensor $\nabla\boldsymbol{u}$ is the covariant derivative of $\boldsymbol{u}$: $(\nabla\boldsymbol{u})_{ij} = \nabla_j u_i$; $\operatorname{tr}(\nabla\boldsymbol{u} \cdot \nabla\boldsymbol{\xi}_1)$ is the trace of the tensor $\nabla\boldsymbol{u} \cdot \nabla\boldsymbol{\xi}_1$ with components $\nabla_k u^i \, \nabla_j \xi_1^k$, and $\nabla\nabla(f)$ is the Hessian of f with components $\nabla_i \nabla_j f$.

3.3. Perturbations of integrals

First, let us denote by r_Σ the mean radius of an interface Σ, by $\boldsymbol{n}$ the unit vector normal to Σ and pointing outward, and by $[f] = f(r_\Sigma^+) - f(r_\Sigma^-)$ the jump of f at the interface in accordance with the orientation of $\boldsymbol{n}$. If a scalar field f, or a vector field $\boldsymbol{u}$, has a jump across the interfaces, an integration by parts gives

$$\int_V \boldsymbol{u} \cdot \operatorname{grad} f \, \mathrm{d}V = -\int_V f \operatorname{div} \boldsymbol{u} \, \mathrm{d}V - \int_\Sigma [f\boldsymbol{u} \cdot \boldsymbol{n}] \, \mathrm{d}\Sigma, \tag{25}$$

where $\int_\Sigma$ involves all interfaces, including the external surface, and where, as a matter of fact, $\int_V$ involves only $V \backslash \Sigma$ where $\operatorname{grad} f$ and $\operatorname{div} \boldsymbol{u}$ are well defined.

To first order, the perturbation of a volume integral $\mathcal{F} = \int_V f(\boldsymbol{x}) \, \mathrm{d}V$, is given by

$$\delta\mathcal{F} = \delta_1\mathcal{F} = \int_{V_0} \delta_{1e} f \, \mathrm{d}V - \int_{\Sigma_0} [f\boldsymbol{\xi}_1 \cdot \boldsymbol{n}] \, \mathrm{d}\Sigma, \tag{26}$$

$$\delta\mathcal{F} = \delta_1\mathcal{F} = \int_{V_0} (\delta_{1l} f + f \operatorname{div} \boldsymbol{\xi}_1) \, \mathrm{d}V, \tag{27}$$

and to second order by

$$\delta\mathcal{F} = \delta_1\mathcal{F} + \frac{1}{2}\delta_2\mathcal{F} \tag{28}$$

with

$$\delta_2\mathcal{F} = \int_{V_0} \{\delta_{2l} f + 2\delta_{1l} f \operatorname{div} \boldsymbol{\xi}_1 + f(\operatorname{div} \boldsymbol{\xi}_2 + (\operatorname{div} \boldsymbol{\xi}_1)^2 - \operatorname{tr}(\nabla\boldsymbol{\xi}_1 \cdot \nabla\boldsymbol{\xi}_1))\} \, \mathrm{d}V. \tag{29}$$

Relations (26) and (27) are classical in continuum mechanics. The proof of (27) relies on the fact that, to first order, the relative change of an elementary volume streamed by the deformation is $\operatorname{div} \boldsymbol{\xi}_1$. The link between (26) and (27) is provided by (22) and (25). Applying (27) twice and using (23) yields (29). Finally, as

$$(\operatorname{div} \boldsymbol{\xi}_1)^2 - \operatorname{tr}(\nabla\boldsymbol{\xi}_1 \cdot \nabla\boldsymbol{\xi}_1) = \operatorname{div}(\boldsymbol{\xi}_1 \operatorname{div} \boldsymbol{\xi}_1 - \nabla\boldsymbol{\xi}_1(\boldsymbol{\xi}_1)), \tag{30}$$

(29) can be rewritten

$$\delta_2\mathcal{F} = \int_{V_0} \delta_{2l} f + 2\delta_{1l} f \operatorname{div} \boldsymbol{\xi}_1 + f \operatorname{div} \left\{\boldsymbol{\xi}_2 + \boldsymbol{\xi}_1 \operatorname{div} \boldsymbol{\xi}_1 - \nabla\boldsymbol{\xi}_1(\boldsymbol{\xi}_1)\right\} \, \mathrm{d}V. \tag{31}$$

4. Perturbation of potential

The perturbation relations can now be applied to Eq. (3) in order to evaluate the perturbation of the gravitational potential. As the shape perturbations correspond to a purely mathematical setting, we are free to choose the evolution of the mapping. It is convenient to choose $\boldsymbol{a}(r, \theta, \lambda)$ as the point of the sphere of radius r with the same θ, λ as $\boldsymbol{x}(r, \theta, \lambda)$ (see Fig. 1). Thus, $\boldsymbol{\xi}_1$ and $\boldsymbol{\xi}_2$ are radial vectors:

$$\boldsymbol{\xi}_1 = \xi_1^r \boldsymbol{e}_\mathrm{r}, \qquad \boldsymbol{\xi}_2 = \xi_2^r \boldsymbol{e}_\mathrm{r}. \tag{32}$$

4.1. Perturbations of ϕ_ℓ^m

We show in Appendix B (Eqs. (B.13) and (B.14)) that the first-order perturbation of the gravitational potential coefficient $\phi_\ell^m = \int_V \rho(r,\theta,\lambda) r^\ell Y_\ell^m(\theta,\lambda)\,\mathrm{d}V$ is

$$\delta_1\phi_\ell^m = \int_{V_0} \delta_{1e}\rho\, r^\ell Y_\ell^m\,\mathrm{d}V - \int_{\Sigma_0} [\rho]\xi_1^r r^\ell Y_\ell^m\,\mathrm{d}\Sigma \quad (33)$$

$$\delta_1\phi_\ell^m = \int_{V_0} (r^\ell \delta_{1l}\rho + \rho\,\mathrm{div}\,(\boldsymbol{\xi}_1 r^\ell)) Y_\ell^m\,\mathrm{d}V, \quad (34)$$

where, for simplicity, we now denote by ρ the reference density $\rho(\boldsymbol{a},0)$. Using Eq. (A.6), relation (33) becomes

$$\delta_1\phi_\ell^m = \int_\Omega \left(\int_0^b \delta_{1e}\rho\, r^{\ell+2}\,\mathrm{d}r - \sum_{r_\Sigma} [\rho]\xi_1^r r^{\ell+2} \right) \times Y_\ell^m\,\mathrm{d}\Omega \quad (35)$$

$$\delta_1\phi_\ell^m = 4\pi \int_0^b \delta_{1e}\rho_\ell^m\, r^{\ell+2}\,\mathrm{d}r - 4\pi \sum_{r_\Sigma} [\rho]\xi_{1\,\ell}^{r\,m} r^{\ell+2}, \quad (36)$$

where $\sum_{r_\Sigma}$ denotes the sum over all interfaces, including the external surface and Ω denotes the unit sphere (see Appendix A). Eq. (36) is commonly used to interpret the global gravity anomalies, either directly (e.g. Ishii and Tromp, 2001, Eq. 5), or after having expressed ξ_1^r as a function of $\delta_{1e}\rho$ through a Newtonian viscous law (e.g. Hager and Clayton, 1989; Ricard and Vigny, 1989).

The total perturbation up to second order is given by (see Appendix B)

$$\delta\phi_\ell^m = \int_{V_0} \{r^\ell \delta_l\rho + \rho\,\mathrm{div}\,(\boldsymbol{\xi} r^\ell)\} Y_\ell^m\,\mathrm{d}V + \int_{V_0} \left\{ \delta_l\rho\,\mathrm{div}\,(\boldsymbol{\xi} r^\ell) + \frac{\ell+2}{2}\rho\ \mathrm{div}(r^{\ell-1}(\xi^r)^2\,\boldsymbol{e}_\mathrm{r}) \right\} Y_\ell^m\,\mathrm{d}V, \quad (37)$$

with (see (19)–(21))

$$\delta\phi_\ell^m = \delta_1\phi_\ell^m + \frac{1}{2}\delta_2\phi_\ell^m, \qquad \boldsymbol{\xi} = \xi^r\boldsymbol{e}_\mathrm{r} = \boldsymbol{\xi}_1 + \frac{1}{2}\boldsymbol{\xi}_2,$$
$$\delta_l\rho = \delta_{1l}\rho + \frac{1}{2}\delta_{2l}\rho. \quad (38)$$

Note that in the quadratic terms, we have replaced $\boldsymbol{\xi}_1$ by $\boldsymbol{\xi}$, since this is correct to second order.

The case when $\ell = 0$ and $Y_\ell^m = Y_0^0 = 1$, corresponds to the perturbation of the mass already considered in Chambat and Valette (2001, Eq. 102). Henceforth, we will only consider $\ell \geq 1$.

4.2. Decomposition into hydrostatic and non-hydrostatic parts

Given a reference density model, we can compute the hydrostatic shape of the corresponding rotating model by integrating Clairaut's equations up to second order (see e.g. Zharkov et al., 1978; Denis, 1989; Moritz, 1990 for a review, and Chambat and Valette, 2001 for a derivation of Clairaut's equation to first order using the shape perturbation formalism).

Let $\xi_\mathrm{h}(r,\theta,\lambda)$ be the height of a hydrostatic equipotential surface with respect to the spherical surface of reference. As equipotential surfaces are also isodensity surfaces, the hydrostatic potential coefficient $\delta_\mathrm{h}\phi_\ell^m$ is obtained by setting $\boldsymbol{\xi} = \xi_\mathrm{h}\boldsymbol{e}_\mathrm{r}$, and $\delta_l\rho = 0$, into expression (37) for $\delta\phi_\ell^m$, i.e.:

$$\delta_\mathrm{h}\phi_\ell^m = \int_{V_0} \left\{ \rho\,\mathrm{div}\,(\xi_\mathrm{h} r^\ell \boldsymbol{e}_\mathrm{r}) + \frac{\ell+2}{2}\rho\ \mathrm{div}\,(\xi_\mathrm{h}^2\, r^{\ell-1}\boldsymbol{e}_\mathrm{r}) \right\} \times Y_\ell^m\,\mathrm{d}V. \quad (39)$$

Let us now decompose ξ_r as follows:

$$\xi_\mathrm{r} = \xi_\mathrm{h} + \xi_\mathrm{d}, \quad (40)$$

where ξ_d is the height above the hydrostatic quasi-ellipsoid and is related to the deviatoric part of the stress tensor. The non-hydrostatic contribution to the potential can now be defined by

$$\delta_\mathrm{d}\phi_\ell^m = \int_{V_0} \{r^\ell \delta_l\rho + \rho\,\mathrm{div}\,(\xi_\mathrm{d} r^\ell \boldsymbol{e}_\mathrm{r})\} Y_\ell^m\,\mathrm{d}V + \int_{V_0} \left\{ \delta_l\rho\,\mathrm{div}\,((\xi_\mathrm{h}+\xi_\mathrm{d}) r^\ell \boldsymbol{e}_\mathrm{r}) + \frac{\ell+2}{2}\rho\ \mathrm{div}(\xi_\mathrm{d}^2\, r^{\ell-1}\boldsymbol{e}_\mathrm{r}) + (\ell+2)\rho\,\mathrm{div}\,(\xi_\mathrm{d}\xi_\mathrm{h}\, r^{\ell-1}\boldsymbol{e}_\mathrm{r}) \right\} Y_\ell^m\,\mathrm{d}V, \quad (41)$$

so that

$$\delta\phi_\ell^m = \delta_\mathrm{h}\phi_\ell^m + \delta_\mathrm{d}\phi_\ell^m. \quad (42)$$

4.3. Specification of ξ_d

The mapping is only constrained at the interfaces where $\boldsymbol{\xi}$ must correspond to the height of the interface with respect to its spherical reference. For simplicity, we consider the limit where $\xi_\mathrm{d} = 0$ between the interfaces. Consequently, $\xi_\mathrm{r} = \xi_\mathrm{h}$, and $\delta_\mathrm{l}\rho$ represent the lateral variations of density over the hydrostatic quasi-ellipsoidal surfaces. As these are non-hydrostatic variations we will denote them by $\delta_\mathrm{d}\rho$.

Because the integrands in Eq. (41) involve derivatives of ξ_d, we perform an integration by parts and take the limit $\xi_\mathrm{d} \to 0$ between the interfaces. On Σ_0, the value of ξ_d is given by the height of the topography above the hydrostatic quasi-ellipsoids. For instance

$$\begin{aligned}&\int_{V_0} \rho\,\mathrm{div}\,(\xi_\mathrm{d} r^\ell \boldsymbol{e}_\mathrm{r}) Y_\ell^m\,\mathrm{d}V\\ &= \int_{V_0} \mathrm{div}\,(\rho\xi_\mathrm{d} r^\ell Y_\ell^m \boldsymbol{e}_\mathrm{r}) - \mathrm{grad}(\rho Y_\ell^m)\cdot \boldsymbol{e}_\mathrm{r}\xi_\mathrm{d} r^\ell\,\mathrm{d}V,\\ &= -\int_{\Sigma_0} [\rho]\xi_\mathrm{d} r^\ell Y_\ell^m\,\mathrm{d}\Sigma - \int_{V_0} (\partial_r\rho)\xi_\mathrm{d} r^\ell Y_\ell^m\,\mathrm{d}V. \end{aligned} \quad (43)$$

By letting $\xi_\mathrm{d} \to 0$ in $V_0\backslash\Sigma_0$, we obtain

$$\int_{V_0} \rho\,\mathrm{div}\,(\xi_\mathrm{d} r^\ell \boldsymbol{e}_\mathrm{r}) Y_\ell^m\,\mathrm{d}V = -\int_{\Sigma_0} [\rho]\xi_\mathrm{d} r^\ell Y_\ell^m\,\mathrm{d}\Sigma. \quad (44)$$

Upon other similar integrations, Eq. (41) can be rewritten

$$\delta_\mathrm{d}\phi_\ell^m = L_\ell^m + A_\ell^m + B_\ell^m + C_\ell^m + D_\ell^m = L_\ell^m + N_\ell^m, \quad (45)$$

with

$$L_\ell^m = \int_{V_0} r^\ell \delta_\mathrm{d}\rho Y_\ell^m\,\mathrm{d}V - \int_{\Sigma_0} [\rho]\xi_\mathrm{d} r^\ell Y_\ell^m\,\mathrm{d}\Sigma, \quad (46)$$

$$A_\ell^m = -\frac{\ell+2}{2}\int_{\Sigma_0} [\rho]\xi_\mathrm{d}^2 r^{\ell-1} Y_\ell^m\,\mathrm{d}\Sigma, \quad (47)$$

$$B_\ell^m = -\int_{\Sigma_0} [\delta_\mathrm{d}\rho]\xi_\mathrm{d} r^\ell Y_\ell^m\,\mathrm{d}\Sigma, \quad (48)$$

$$\begin{aligned}C_\ell^m = &\int_{V_0} \delta_\mathrm{d}\rho\,\mathrm{div}\,(\xi_\mathrm{h} r^\ell \boldsymbol{e}_\mathrm{r}) Y_\ell^m\,\mathrm{d}V\\ &-(\ell+3)\int_{\Sigma_0} [\rho]\xi_\mathrm{d}\xi_\mathrm{h} r^{\ell-1} Y_\ell^m\,\mathrm{d}\Sigma,\end{aligned} \quad (49)$$

$$D_\ell^m = \int_{\Sigma_0} [\rho]\xi_\mathrm{d}\xi_\mathrm{h} r^{\ell-1} Y_\ell^m\,\mathrm{d}\Sigma. \quad (50)$$

L_ℓ^m is the term classically considered in the linear theory (Eq. (33)), the inversion of which provides constraints on density heterogeneity within the Earth. The remaining second-order terms should be subtracted from the observed potential if one wished to preserve the linear inversion formalism. They will be numerically estimated in the next section. A_ℓ^m corresponds to a piecewise homogeneous Earth model (Balmino, 1994). Note that in A_ℓ^m, the contributions from the outer surface and the Moho sum up, whereas they cancel each other in L_ℓ^m. B_ℓ^m accounts for the coupling of non-hydrostatic topography and lateral variations of density over the interfaces. To our knowledge, the terms C_ℓ^m and D_ℓ^m have never been considered before. They represent the coupling between hydrostatic shape and non-hydrostatic structure. The decomposition into C_ℓ^m and D_ℓ^m has been chosen in order to obtain expressions that can be easily evaluated (see Sections 5.3 and 5.4). N_ℓ^m is the sum of all the non-linear terms.

5. Numerical evaluations

In order to compare the non-linear terms to the observed potential models available up to $\ell = 360$, density and topographic models are needed. As such a high resolution is only reached for the external topography, we will use approximations that should be sufficient to evaluate the order of magnitude of these correcting terms.

The height and gravity anomalies corresponding to A_ℓ^m, B_ℓ^m, C_ℓ^m, D_ℓ^m, N_ℓ^m, are defined by introducing these quantities instead of ϕ_ℓ^m in relations (8) and (9), and are denoted by $\zeta_{A\ell}^m$, $\zeta_{B\ell}^m$, $\zeta_{C\ell}^m$, $\zeta_{D\ell}^m$, $\zeta_{N\ell}^m$ and $\delta_A g_\ell^m$, $\delta_B g_\ell^m$, $\delta_C g_\ell^m$, $\delta_\mathrm{D} g_\ell^m$, $\delta_N g_\ell^m$.

Denoting by ζ_obs the observed value, we define, for each ℓ, the scalar product with a second-order term, say ζ_A, by $\langle\zeta_\mathrm{obs}, \zeta_A\rangle_\ell = \sum_{m=-\ell}^{\ell} \zeta_{\mathrm{obs}\,\ell}^m \zeta_{A\ell}^m$. We will compare the second-order terms with the observed values through the ratio of their norm:

$$\frac{\|\zeta_A\|_\ell}{\|\zeta_{\rm obs}\|_\ell} = \frac{\sqrt{\langle \zeta_A, \zeta_A\rangle_\ell}}{\sqrt{\langle \zeta_{\rm obs}, \zeta_{\rm obs}\rangle_\ell}}, \tag{51}$$

the correlation:

$$\mathrm{Cor}_\ell(\zeta_{\rm obs}, \zeta_A) = \frac{\langle \zeta_{\rm obs}, \zeta_A\rangle_\ell}{\|\zeta_{\rm obs}\|_\ell \|\zeta_A\|_\ell}, \tag{52}$$

and the variance reduction:

$$V_\ell(\zeta_{\rm obs}, \zeta_A) = \frac{\|\zeta_{\rm obs}\|_\ell^2 - \|\zeta_{\rm obs} - \zeta_A\|_\ell^2}{\|\zeta_{\rm obs}\|_\ell^2}. \tag{53}$$

Notice that these three quantities are invariant when replacing ζ_A and $\zeta_{\rm obs}$ by $\delta_A g$ and $\delta g_{\rm obs}$, or by $\phi_{\rm obs}$ and A, respectively.

5.1. The A_ℓ^m term

Using (A.4), we rewrite A_ℓ^m as

$$A_\ell^m = -2\pi(\ell+2)\sum_{r_\Sigma} r_\Sigma^{\ell+1}[\rho](\xi_{\rm d}^2)_\ell^m(r_\Sigma). \tag{54}$$

The coefficients $(\xi_{\rm d}^2)_\ell^m$ of the squared topographies can be evaluated from models of interfaces by direct integration over the sphere. These digital elevation models provide estimations of the altitude of the interfaces, i.e. the height H of the interface with respect to the quasi-geoid. We identify H with $\xi_{\rm d}$, the height with respect to the hydrostatic quasi-ellipsoid. The harmonic component of degree zero of $\xi_{\rm d}$ is null, i.e. $\xi_{\rm d}(\theta,\lambda) = H(\theta,\lambda) - H_0^0$, because, by definition, the radii of the reference model are the mean radii of the Earth (Chambat and Valette, 2001).

Owing to $r_\Sigma/b < 1$ and to the likely amplitudes of $[\rho]\xi_{\rm d}^2$, the main contribution to A_ℓ^m comes from crustal topographies. Thus, we ignore the discontinuities at 410 km, 660 km, and at the CMB. Going downward, we consider four interfaces and five layers: atmosphere ($\rho = 0$), ice ($\rho_{\rm i} = 900\,{\rm kg/m^3}$), oceanic water ($\rho_{\rm w} = 1000\,{\rm kg/m^3}$), crust ($\rho_{\rm c} = 2900\,{\rm kg/m^3}$), and mantle ($\rho_{\rm m} = 3250\,{\rm kg/m^3}$). The four corresponding topographies are, respectively, denoted by $\xi_{\rm d}^{\rm out}$ for the outer topography, $\xi_{\rm d}^{\rm ice}$ for the bottom of ice, $\xi_{\rm d}^{\rm rock}$ for the top of solid rock (bottom of water and ice), and $\xi_{\rm d}^{\rm Moho}$ for the Moho. The first three are directly given by the digital elevation model JGP95E (e.g. EGM96 web site[1]).

For A_ℓ^m, the Moho topography can be evaluated under the Airy's isostatic hypothesis $\sum_{r_\Sigma}[\rho]\xi_{\rm d} = 0$, i.e.

$$\xi_{\rm d}^{\rm Moho} = -\frac{\rho_{\rm c}}{\rho_{\rm m} - \rho_{\rm c}}\xi^{\rm eq}, \tag{55}$$

where the equivalent rock topography $\xi^{\rm eq}$ is defined by

$$\rho_{\rm c}\xi^{\rm eq} = \rho_{\rm c}\xi_{\rm d}^{\rm rock} + \rho_{\rm w}(\xi_{\rm d}^{\rm ice} - \xi_{\rm d}^{\rm rock}) + \rho_{\rm i}(\xi_{\rm d}^{\rm out} - \xi_{\rm d}^{\rm ice}) \tag{56}$$

in order to replace the water and ice by a mass-equivalent crustal layer (Balmino et al., 1973).

This leads to the corresponding height and gravity anomalies (8)–(9):

$$\zeta_{A\ell}^m = -\frac{3(\ell+2)}{2(2\ell+1)}\sum_{r_\Sigma}\left(\frac{r_\Sigma}{b}\right)^{\ell+1}\frac{[\rho]}{\rho_2}\frac{(\xi_{\rm d}^2)_\ell^m}{b}(r_\Sigma), \tag{57}$$

$$\frac{\delta_A g_\ell^m}{g} = (\ell-1)\frac{\zeta_{Al}^m}{b}, \tag{58}$$

where r_Σ denotes the mean radii of the four topographies mentioned above. These relations, together with (55), enable us to evaluate ζ_A and $\delta_A g$.

Figs. 2 and 4 show maps of $\delta_A g$ and ζ_A. Their values are significant in high topography regions, namely Tibet and Andes, where the height reaches 30 m and 15 m, respectively, and the gravity reaches 80 mgal. These values are comparable with those derived from the geopotential model EGM96 (Lemoine et al., 1998) and shown in Figs. 3 and 5.

For $\ell \gtrsim 15$, A_ℓ^m is well correlated to the observed potential (Fig. 6) and yields a 40% norm ratio (Fig. 7). For $\ell = 20$–60, this term contributes up to 30% in the observed potential variance (Fig. 8).

Note also that, under the approximations $(\ell+2)/(2\ell+1) \simeq 1/2$ and $(r_\Sigma/b)^{\ell+1} \simeq 1$, the following local relation holds:

$$\zeta_A \simeq \frac{3}{4\rho_2 b}\sum_{r_\Sigma}[\rho]\xi_{\rm d}^2(r_\Sigma). \tag{59}$$

Considering only the equivalent rock topography and Moho yields

[1] ftp://cddisa.gsfc.nasa.gov/pub/egm96/.

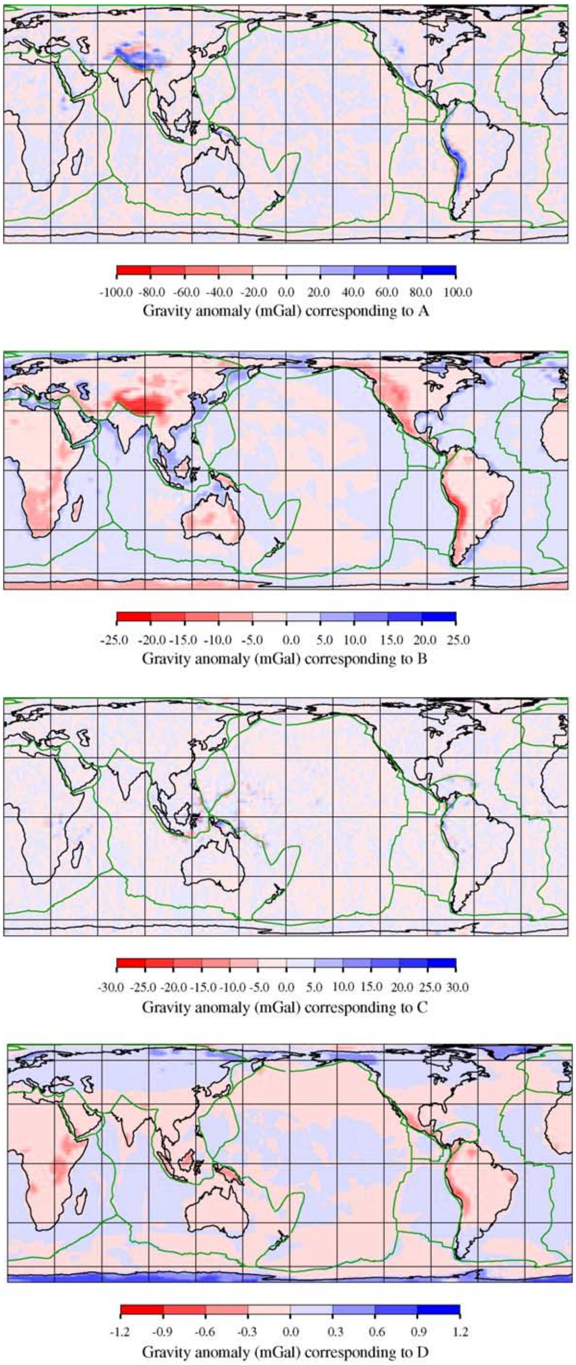

Fig. 2. Gravity anomalies δg. The four maps correspond to the terms A, B, C, and D, respectively. Notice that the color scales are not the same for all the drawings.

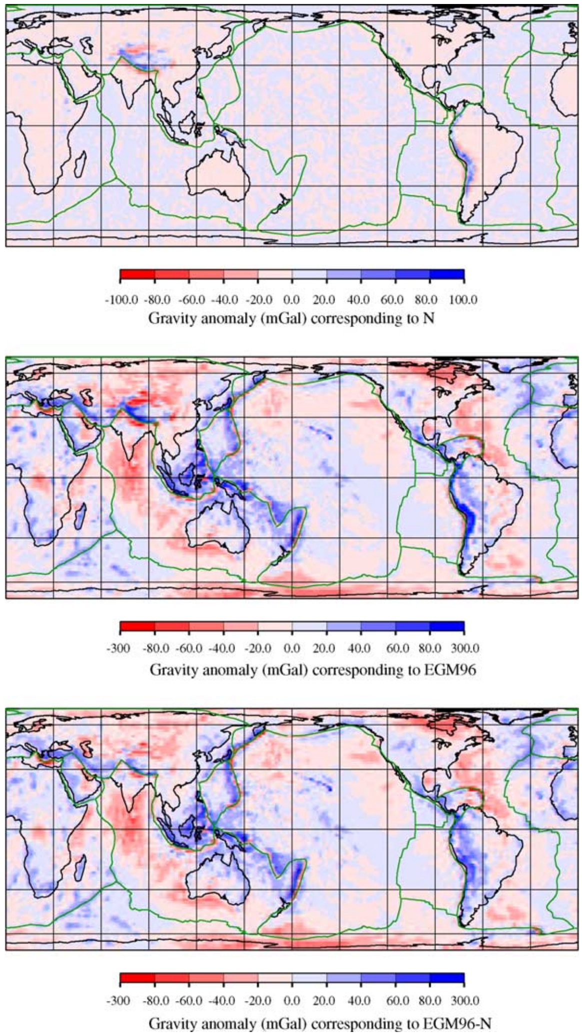

Fig. 3. Gravity anomalies δg. The three maps show the global non-linear contribution N to the gravity, the EGM96 model, and EGM96 corrected with the non-linear term. Notice that the color scales are not the same for all the drawings and that the intervals do not always have a constant length within a scale.

$$\frac{\zeta_A}{b} \simeq -\frac{3\rho_c}{4\rho_2}\left(1+\frac{\rho_c}{\rho_m-\rho_c}\right)\left(\frac{\xi^{eq}}{b}\right)^2 \simeq 4\left(\frac{\xi^{eq}}{b}\right)^2. \tag{60}$$

It shows that the term $\rho_c/(\rho_m-\rho_c) \simeq 8$ corresponding to the Moho is dominant and that A_ℓ^m is significant in high topography regions.

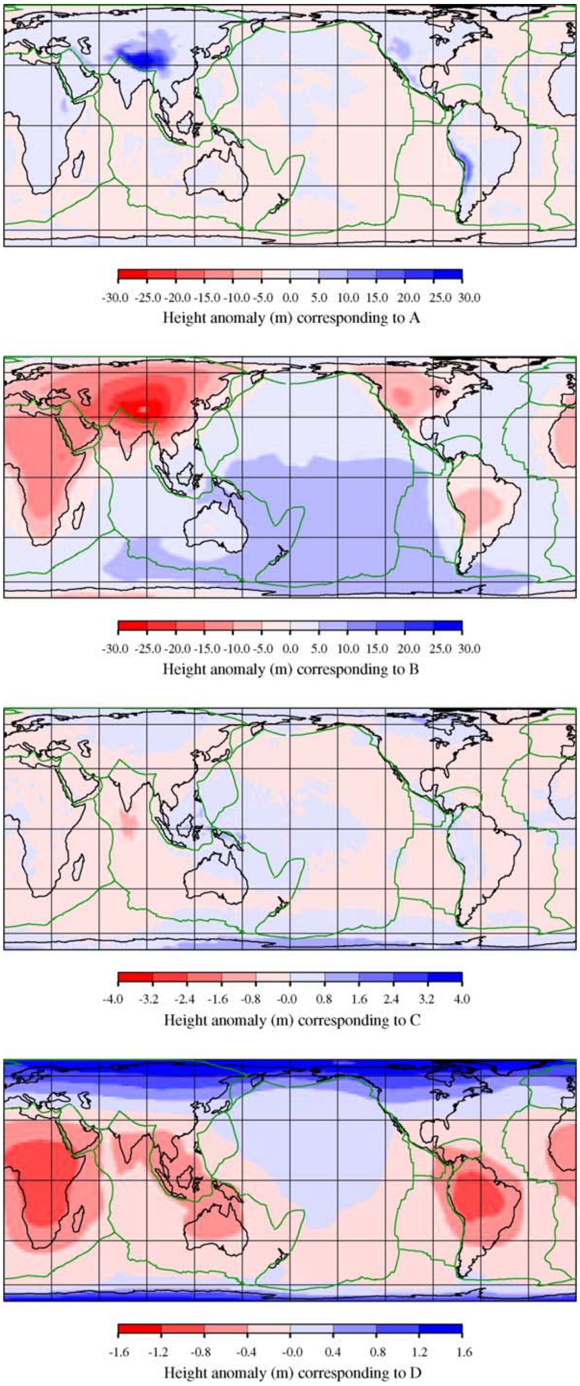

Fig. 4. Same as Fig. 2 for height anomalies (ζ).

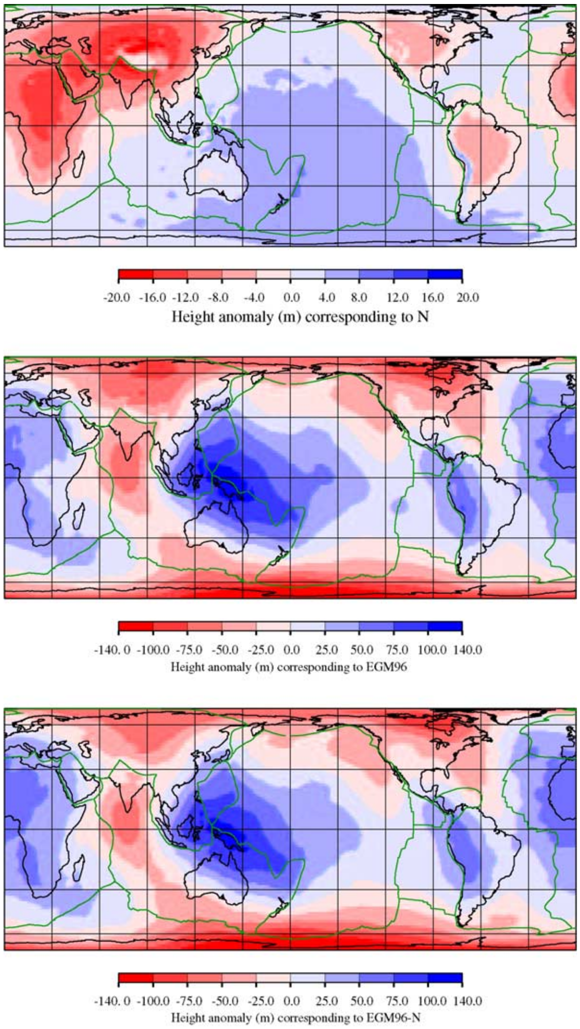

Fig. 5. Same as Fig. 3 for height anomalies (ζ).

5.2. The B_ℓ^m term

B_ℓ^m is given by

$$B_\ell^m = -4\pi \sum_{r_\Sigma} r_\Sigma^{\ell+2} ([\delta_\mathrm{d}\rho]\xi_\mathrm{d})_\ell^m, \tag{61}$$

and the corresponding height anomaly is

$$\zeta_{B\ell}^m = -\frac{3}{2\ell+1} \sum_{r_\Sigma} \left(\frac{r_\Sigma}{b}\right)^{\ell+2} \frac{([\delta_\mathrm{d}\rho]\xi_\mathrm{d})_\ell^m}{\rho_2}. \tag{62}$$

Assuming that the lateral variations of density over the Moho can be neglected, we consider the contribution

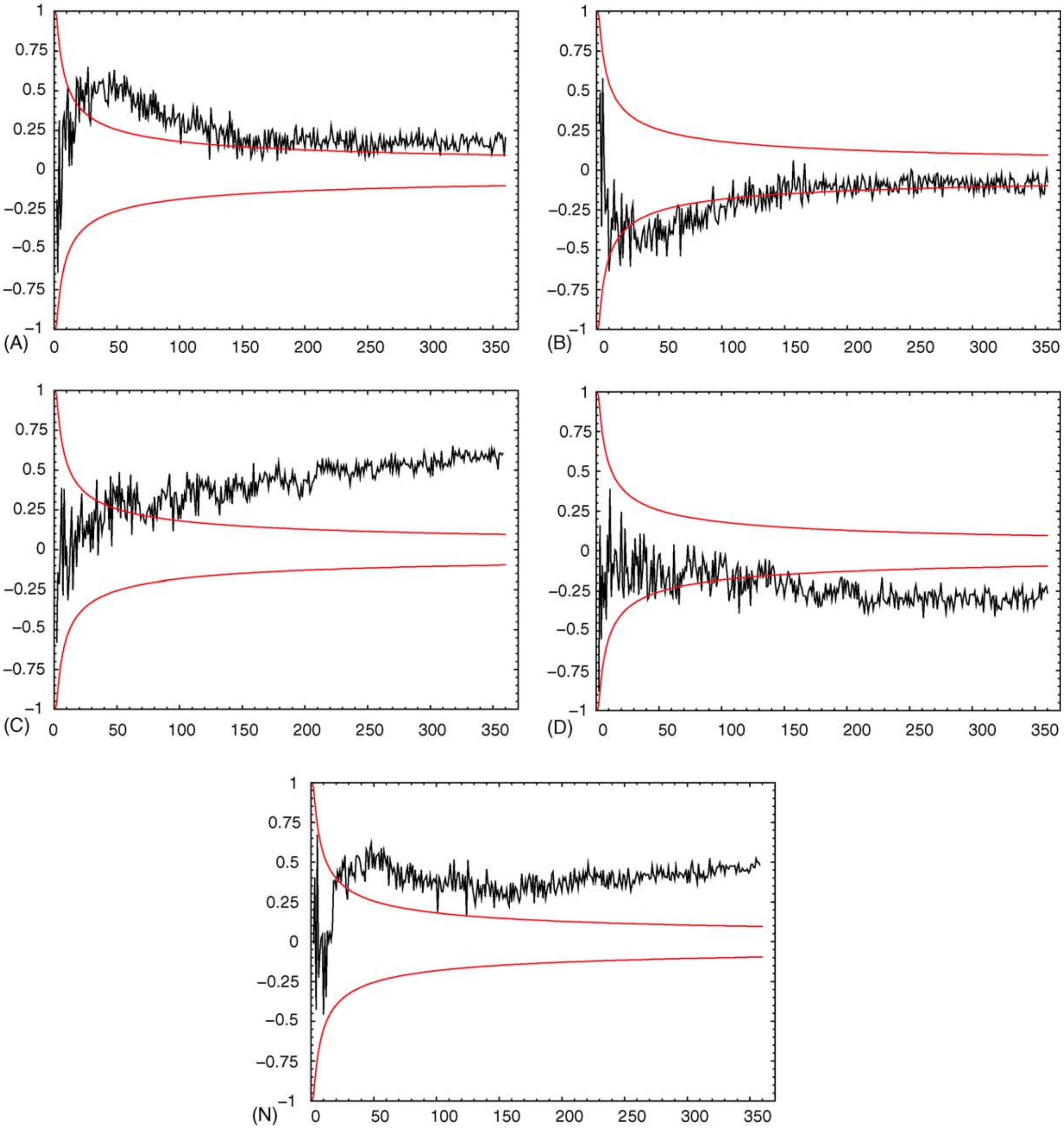

Fig. 6. Correlation, as a function of ℓ (cf. Eq. (52)), of the second-order terms with EGM96. The dotted line is the 99% confidence level.

of the equivalent topography only. At the outer surface, we assume that the density is proportional to the ocean–continent function O_c defined by $O_c = 1$ in the oceanic domain and $O_c = 0$ on the continental domain. Defining $\Delta\rho$ as the difference between the densities of the oceanic and continental crusts and taking into account that the degree zero component of the perturbation of density is null, we have

$$\delta_d\rho = \Delta\rho(O_c - (O_c)_0^0). \tag{63}$$

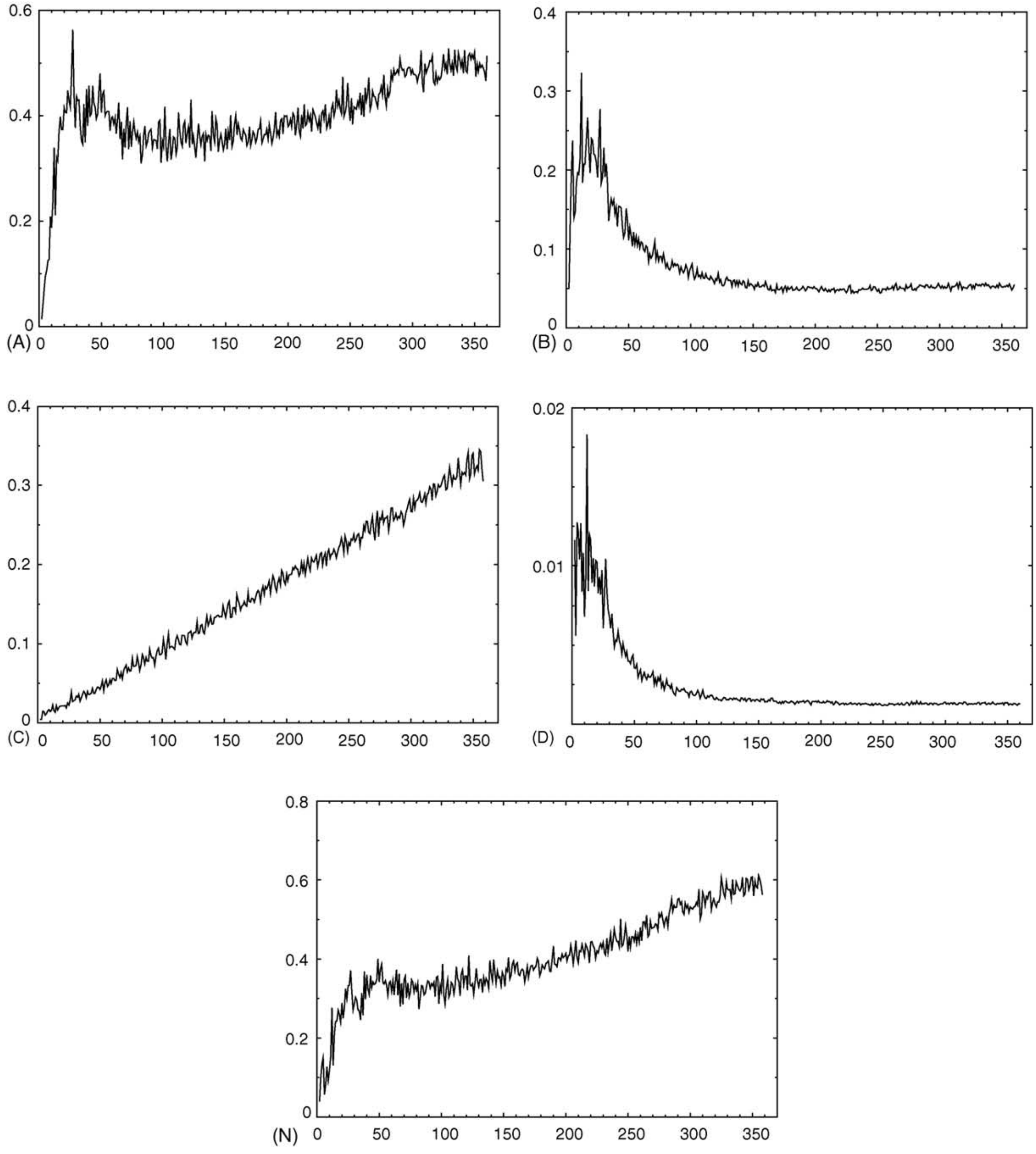

Fig. 7. Norm ratio with respect to EGM96, as a function of ℓ (cf. Eq. (51)), of the second-order terms.

Thus, the height anomaly is

$$\zeta_{B\ell}^{m} = \frac{3}{2\ell+1}\frac{\Delta\rho}{\rho_2}((O_\mathrm{c} - (O_\mathrm{c})_0^0)\xi^{\mathrm{eq}})_\ell^m. \qquad (64)$$

Taking $\Delta\rho = 150\,\mathrm{kg/m^3}$ we obtain gravity and height anomalies ranging from -25 mgal to 12 mgal and -30 m to 10 m, respectively (Figs. 2 and 4). $\delta_B g$ is anti-correlated with the observed gravity. This is more

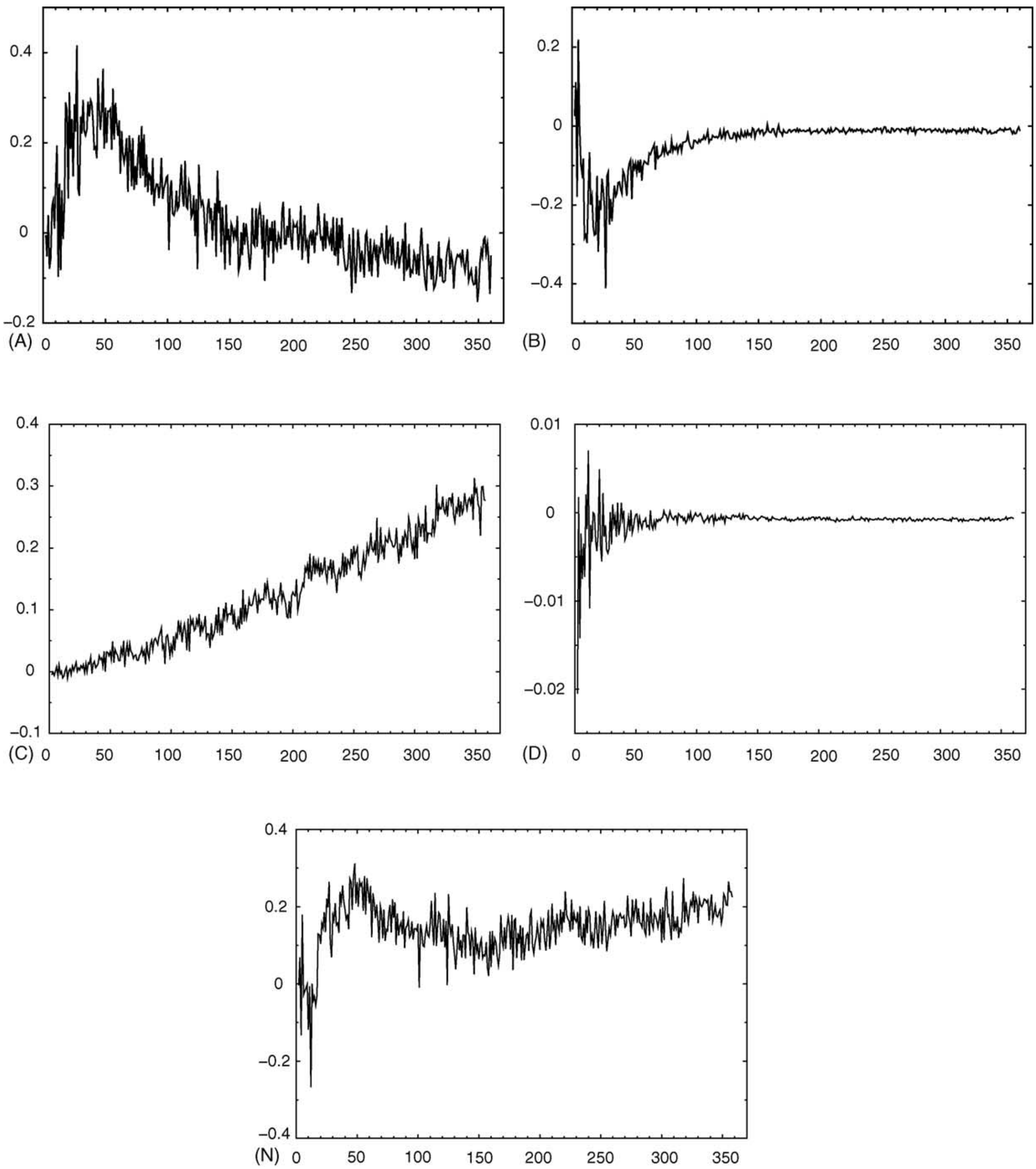

Fig. 8. EGM96 variance reduction, as a function of ℓ (cf. Eq. (53)), due to the second-order terms. A reduction of 0.1 means that the second order explains 10% of the data variance.

obvious in the spectral domain where the correlation is negative for $\ell \gtrsim 7$ (Fig. 6). This implies that the variance reduction is negative (Fig. 8), which means that this term does not explain at all the observed potential. However, B_ℓ^m should cancel with terms in L_ℓ^m because of isostasy. We have indeed

$$L_\ell^m + B_\ell^m = \int_{V_0} r^\ell \delta_\mathrm{d}\rho Y_\ell^m \,\mathrm{d}V - \int_{\Sigma_0} [\rho + \delta_\mathrm{d}\rho]\xi_\mathrm{d} r^\ell Y_\ell^m \,\mathrm{d}\Sigma \tag{65}$$

$$L_\ell^m + B_\ell^m = \int_\Omega \left(\int_0^b \delta_\mathrm{d}\rho\, r^{\ell+2}\,\mathrm{d}r - \sum_{r_\Sigma} [\rho + \delta_\mathrm{d}\rho]\xi_\mathrm{d} r_\Sigma^{\ell+2} \right) \times Y_\ell^m \,\mathrm{d}\Omega. \tag{66}$$

Considering $r \simeq$ cste in the uppermost part of the Earth, isostasy states that the expression inside the parenthesis is small.

5.3. The C_ℓ^m term

Let us now evaluate the order of magnitude of the first term that couples the hydrostatic shape with the non-hydrostatic perturbations (Eq. 49). Correct to first order, the hydrostatic shape is (e.g. Chambat and Valette, 2001)

$$\xi_\mathrm{h}(r, \theta, \lambda) = -\frac{2}{3\sqrt{5}} r\epsilon(r) Y_2^0(\theta, \lambda), \tag{67}$$

where ϵ is the flattening of the hydrostatic quasi-ellipsoids. As the flattening does not vary much within the Earth, and as the non-hydrostatic perturbations occur mainly in the uppermost part of the Earth, it is sufficient to use the approximation $\epsilon(r) \simeq \epsilon(b) \simeq 1/300$. Substituting (67) into (49) yields

$$C_\ell^m = -\frac{2}{3\sqrt{5}}\epsilon(b)(\ell+3) \times \left(\int_{V_0} \delta_\mathrm{d}\rho\, r^\ell Y_2^0 Y_\ell^m \,\mathrm{d}V - \int_{\Sigma_0} [\rho]\xi_\mathrm{d} r^\ell Y_2^0 Y_\ell^m \,\mathrm{d}\Sigma \right) \tag{68}$$

$$C_\ell^m = -\frac{2}{3\sqrt{5}}\epsilon(b)(\ell+3) \int_\Omega \left(\int_0^b \delta_\mathrm{d}\rho\, r^{\ell+2}\,\mathrm{d}r - \sum_{r_\Sigma} [\rho]\xi_\mathrm{d} r_\Sigma^{\ell+2} \right) Y_2^0 Y_\ell^m \,\mathrm{d}\Omega. \tag{69}$$

The comparison of expression (68) for C_ℓ^m with expression (46) for L_ℓ^m suggests that, owing to the additional factor Y_2^0 in (68), C_ℓ^m can be approximately expressed as a function of L_ℓ^m, $L_{\ell-2}^m$ and $L_{\ell+2}^m$. More precisely, if we assume that $(r/b)^2 \simeq 1$ in the uppermost part of the Earth, we show in Appendix C that an approximate expression for the corresponding height anomaly is

$$\zeta_{C\ell}^m = -\frac{\epsilon(b)}{6\pi\sqrt{5}} \frac{\ell+3}{2\ell+1} b \int_\Omega \left(2\frac{\delta_\mathrm{d} g}{g} + 3\frac{\zeta_\mathrm{d}}{b} \right) Y_2^0 Y_\ell^m \,\mathrm{d}\Omega \tag{70}$$

where ζ_d and $\delta_\mathrm{d} g$ are the first-order non-hydrostatic height and gravity anomalies, defined by (8) and (9), with L_ℓ^m instead of ϕ_ℓ^m. Approximating these first-order anomalies with the observed values, we find that the $\delta_C g$ and ζ_C ranges are −70 mgal, 60 mgal, and ±4 m (Figs. 2 and 4). The spectral amplitude reaches 35% of the observed one at high degrees, the variance reduction reaching 30% (Figs. 7 and 8). The growth of the ratio of second order to observed potential with ℓ (Fig. 7) indicates that taking the observed values for ζ_d and $\delta_\mathrm{d} g$ is a good approximation for relatively low ℓ only.

Note also that, assuming $(\ell+3)/(2\ell+1) \simeq 1/2$, we can deduce from (70) the local relation

$$\zeta_C(\theta, \lambda) = -\frac{\epsilon(b)}{3\sqrt{5}} b \left(2\frac{\delta_\mathrm{d} g(\theta, \lambda)}{g} + 3\frac{\zeta_\mathrm{d}(\theta, \lambda)}{b} \right) Y_2^0(\theta, \lambda) \tag{71}$$

$$\zeta_C(\theta, \lambda) = \xi_\mathrm{h}(b, \theta, \lambda) \left(\frac{\delta_\mathrm{d} g(\theta, \lambda)}{g} + \frac{3\zeta_\mathrm{d}(\theta, \lambda)}{2b} \right). \tag{72}$$

5.4. The D_ℓ^m term

Substituting (67) into the expression (50) of D_ℓ^m and using $\epsilon(r) \simeq \epsilon(b)$ yield

$$D_\ell^m = -\frac{2}{3\sqrt{5}}\epsilon(b)\int_\Omega\left(\sum_{r_\Sigma}[\rho]\xi_\mathrm{d} r_\Sigma^{\ell+2}\right)Y_2^0 Y_\ell^m\,\mathrm{d}\Omega. \tag{73}$$

Under the assumption $r_\Sigma^{\ell+2} \simeq b^{\ell+2}$, the Airy compensation $\sum_{r_\Sigma}[\rho]\xi_\mathrm{d} = 0$ would imply that D_ℓ^m is very small. A more convenient hypothesis is to restrict the Airy compensation to the continental area and to assume a constant crustal oceanic thickness ($\sum_{r_\Sigma}[\rho]\xi_\mathrm{d} = -\rho_\mathrm{m}\xi^\mathrm{eq} O_\mathrm{c}$). It yields for the height anomaly:

$$\zeta_{D\ell}^m = \frac{\epsilon(b)}{2\pi\sqrt{5}(2\ell+1)}\frac{\rho_\mathrm{m}}{\rho_2}\int_\Omega(\xi^\mathrm{eq} O_\mathrm{c} - (\xi^\mathrm{eq} O_\mathrm{c})_0^0)Y_2^0 Y_\ell^m\,\mathrm{d}\Omega. \tag{74}$$

We find that the corresponding gravity is less than 1.2 mgal and the height is less than 1.6 m (Figs. 2 and 4). The spectral amplitude is less than 2% of the observed one, and the variance reduction less than 2% (Figs. 7 and 8). This term is the smallest one and is negligible.

5.5. The N_ℓ^m sum

Let us now consider the N_ℓ^m sum of all the second-order terms. $\delta_N g$ ranges from −135 mgal to 220 mgal, while ζ_N varies from −19 m to 12 m (Figs. 3 and 5). The norm ratio reaches 60% at high degrees while the variance reduction is about 20% for $\ell \gtrsim 20$ (Figs. 7 and 8). The variance is reduced mainly by the *A* term, and, to a lesser extent, by the *C* term at high degrees.

The influence of the second-order terms is weak at low degrees. For example, the $(\ell, m) = (2, 0)$ values, $\zeta_{A2}^0 = 0.03$ m, $\zeta_{B2}^0 = -0.15$ m, $\zeta_{C2}^0 = 0.13$ m, and $\zeta_{D2}^0 = 0.44$ m are small with respect to the observed non-hydrostatic value of 33 m.

Note that these four terms are probably not estimated with the same accuracy. Our estimation of A_ℓ^m, which is the predominant term, is fairly accurate, at least for relatively low degrees for which the Airy compensation is a good approximation. C_ℓ^m is the most accurately computed term since its calculation relies on very few hypotheses. Because this term involves the first-order potential, its computation could still be improved by using an iterative procedure. B_ℓ^m an D_ℓ^m are less accurately determined, but D_ℓ^m is negligible and B_ℓ^m is only significant at low degrees.

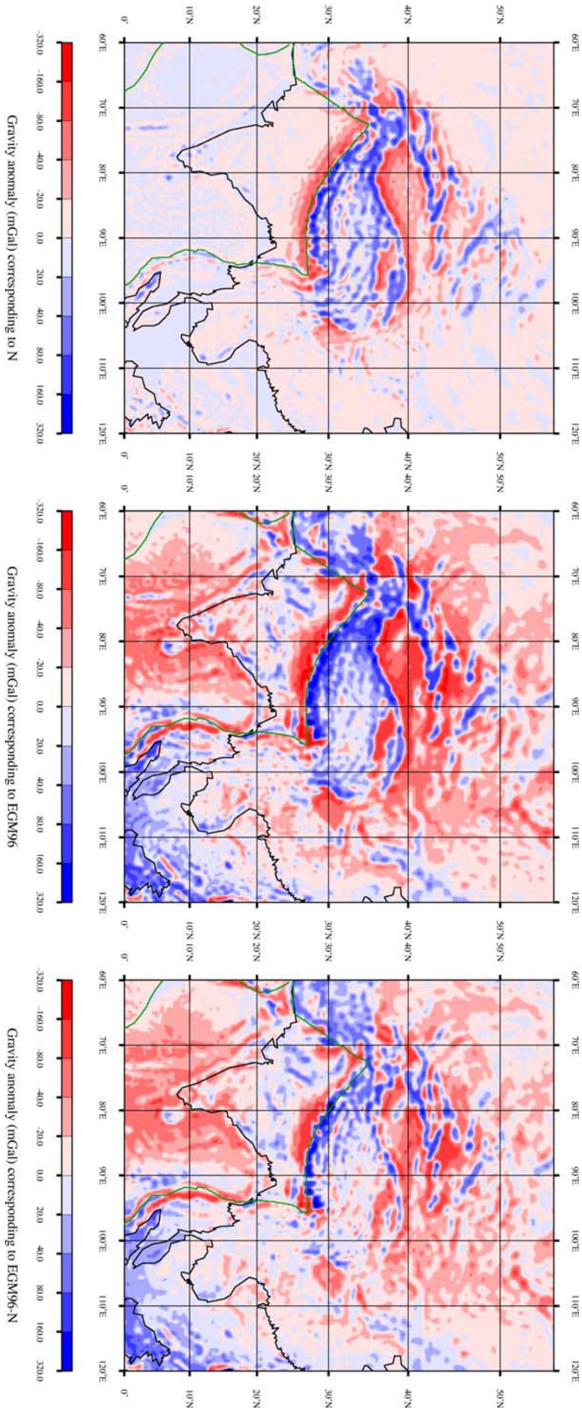

Fig. 9. Detail of the gravity anomaly (mgal) in Tibet. From left to right: non-linear contribution (*N*), EGM96 gravity, and EGM96 corrected with the non-linear term. Notice that the intervals do not have a constant length within the scale.

6. Conclusion

Usually, in order to constrain the Earth's internal structure, the potential is interpreted by using its first-order expression as a function of density lateral variations and topography. We have here extended these expressions up to second-order. The magnitude of this second-order potential has been evaluated up to harmonic degree $\ell = 360$. For $\ell \gtrsim 20$, its amplitude is about 30% of the observed potential, yielding a 20% variance reduction. Maps of the difference between the observed potential and its second-order estimation illustrate this variance reduction in the spatial domain (Figs. 3 and 5). The second-order term accounts for a significant part of the gravity field over Tibet and the Andes (Figs. 3 and 9); it reaches 20 m in terms of height anomaly.

Our numerical evaluation also shows that, for low harmonic degrees, the influence of the non-linear term is relatively small. As a consequence, global Earth models that are constrained by the lower harmonic degrees of the gravitational field only, would not be dramatically modified by taking non-linear terms into account. On the contrary, second-order terms significantly contribute to the gravitational potential for intermediate wavelengths ($20 \lesssim \ell \lesssim 360$). Thus, when trying to constrain the interior of the Earth, or any planet, global inversions of the complete gravity dataset should incorporate the non-linear terms discussed in this article.

Acknowledgements

We are grateful to Yves Rogister, Emmanuel Chaljub, and Yanick Ricard for careful reviews of a draft of the article.

Appendix A. Definition of Y_ℓ^m

We use the real spherical harmonics, defined for $\ell, m \in \mathbb{N}$, $-\ell \le m \le \ell$ by

$$Y_\ell^m(\theta,\lambda) = \begin{cases} p_\ell^m(\cos\theta)\cos(m\lambda), & \text{if } m \ge 0, \\ p_\ell^{|m|}(\cos\theta)\sin(|m|\lambda), & \text{if } m < 0 \end{cases} \quad \text{(A.1)}$$

where p_ℓ^m is the Legendre function of degree ℓ and order m, with the following normalization:

$$\begin{aligned} &\frac{1}{4\pi}\int_\Omega Y_\ell^m(\theta,\lambda)Y_{\ell'}^{m'}(\theta,\lambda)\,\mathrm{d}\Omega \\ &= \frac{1}{4\pi}\int_0^{2\pi}\int_0^{\pi} Y_\ell^m(\theta,\lambda)Y_{\ell'}^{m'}(\theta,\lambda)\sin\theta\,\mathrm{d}\theta\,\mathrm{d}\lambda \\ &= \delta_\ell^{\ell'}\delta_m^{m'}, \end{aligned} \quad \text{(A.2)}$$

where δ_i^j is the Kronecker symbol and where Ω denotes the unit sphere. This yields for instance:

$$\begin{aligned} &Y_0^0(\theta,\lambda) = 1, \qquad Y_1^0(\theta,\lambda) = \sqrt{3}\cos\theta, \\ &Y_1^1(\theta,\lambda) = \sqrt{3}\sin\theta\cos\lambda, \\ &Y_1^{-1}(\theta,\lambda) = \sqrt{3}\sin\theta\sin\lambda, \\ &Y_2^0(\theta,\lambda) = \frac{\sqrt{5}}{2}(3\cos^2\theta - 1). \end{aligned} \quad \text{(A.3)}$$

The degree ℓ, order m, coefficient of a function $h(\theta,\lambda)$ is denoted by h_ℓ^m:

$$h_\ell^m = \frac{1}{4\pi}\int_\Omega h(\theta,\lambda)Y_\ell^m(\theta,\lambda)\,\mathrm{d}\Omega, \quad \text{(A.4)}$$

$$h(\theta,\lambda) = \sum_{\ell=0}^{\infty}\sum_{m=-\ell}^{\ell} h_\ell^m Y_\ell^m(\theta,\lambda). \quad \text{(A.5)}$$

For a field $h(r,\theta,\lambda)$ defined in a spherical volume V_0, Eq. (A.4) yields

$$\begin{aligned} \int_{V_0} hY_\ell^m\,\mathrm{d}V &= \int_0^b\int_\Omega hY_\ell^m\,\mathrm{d}\Omega r^2\,\mathrm{d}r \\ &= 4\pi\int_0^b h_\ell^m(r)r^2\,\mathrm{d}r. \end{aligned} \quad \text{(A.6)}$$

Appendix B. Perturbations of $\int_V f(x)r^kY_\ell^m\mathrm{d}V$

In this appendix, we first show that the perturbations of volume integrals of the kind

$$\mathcal{F} = \int_V f(x)r^k\,\mathrm{d}V \quad \text{(B.1)}$$

are given, to first order, by

$$\delta_1\mathcal{F} = \int_{V_0} r^k \delta_{1e} f \,\mathrm{d}V - \int_{\Sigma_0} r^k [f\boldsymbol{\xi}_1 \cdot n]\,\mathrm{d}\Sigma, \qquad \text{(B.2)}$$

$$\delta_1\mathcal{F} = \int_{V_0} (r^k \delta_{1l} f + f \operatorname{div}(r^k \boldsymbol{\xi}_1))\,\mathrm{d}V, \qquad \text{(B.3)}$$

and to second order by

$$\delta_2\mathcal{F} = \int_{V_0} \{r^k \delta_{2l} f + 2\delta_{1l} f \operatorname{div}(r^k \boldsymbol{\xi}_1) + f \operatorname{div}(r^k \boldsymbol{\xi}_2) + f \operatorname{div}(r^k \boldsymbol{\xi}_1 \operatorname{div} \boldsymbol{\xi}_1 - r^k \nabla\boldsymbol{\xi}_1(\boldsymbol{\xi}_1) + \operatorname{grad}(r^k)\cdot\boldsymbol{\xi}_1\,\boldsymbol{\xi}_1)\}\,\mathrm{d}V. \qquad \text{(B.4)}$$

When $\boldsymbol{\xi}_1$ is radial, this expression can be simplified in

$$\delta_2\mathcal{F} = \int_{V_0} \{r^k \delta_{2l} f + 2\delta_{1l} f \operatorname{div}(r^k \boldsymbol{\xi}_1) + f(\operatorname{div}(r^k \boldsymbol{\xi}_2) + (k+2)) f \operatorname{div}(\boldsymbol{\xi}_1\cdot\boldsymbol{\xi}_1 r^{k-1}\boldsymbol{e}_\mathrm{r})\}\,\mathrm{d}V. \qquad \text{(B.5)}$$

In order to show these relations, we first notice that since r is constant at a fixed point during the evolution

$$\delta_{1e} r^k = 0 \quad \text{and} \quad \delta_{2e} r^k = 0. \qquad \text{(B.6)}$$

Thus, relation (22) implies that

$$\delta_{1l} r^k = \operatorname{grad}(r^k)\cdot\boldsymbol{\xi}_1. \qquad \text{(B.7)}$$

Using (24) and (15), we deduce that

$$\delta_{2l} r^k = \delta_{1l}(\operatorname{grad}(r^k)\cdot\boldsymbol{\xi}_1) = \operatorname{grad}(r^k)\cdot\boldsymbol{\xi}_2 + \nabla\nabla(r^k)(\boldsymbol{\xi}_1)\cdot\boldsymbol{\xi}_1. \qquad \text{(B.8)}$$

The definitions of perturbations as derivatives yield

$$\delta_{1l}(r^k f) = r^k \delta_{1l} f + f\delta_{1l} r^k, \qquad \text{(B.9)}$$

$$\delta_{2l}(r^k f) = r^k \delta_{2l} f + 2(\delta_{1l} r^k)(\delta_{1l} f) + f\delta_{2l} r^k. \qquad \text{(B.10)}$$

Now substituting (B.6) into (26) yields (B.2), and substituting (B.7) and (B.9) into (27) yields (B.3). Substituting (B.6)–(B.10) into (31) yields

$$\delta_2\mathcal{F} = \int_{V_0} \{r^k \delta_{2l} f + 2\delta_{1l} f \operatorname{div}(r^k \boldsymbol{\xi}_1) + f(\operatorname{div}(r^k \boldsymbol{\xi}_2) + r^k \operatorname{div}(\boldsymbol{\xi}_1 \operatorname{div}\boldsymbol{\xi}_1 - \nabla\boldsymbol{\xi}_1(\boldsymbol{\xi}_1))) + f\nabla\nabla(r^k)\boldsymbol{\xi}_1\cdot\boldsymbol{\xi}_1 + 2f\operatorname{grad}(r^k)\cdot\boldsymbol{\xi}_1 \operatorname{div}\boldsymbol{\xi}_1\}\,\mathrm{d}V. \qquad \text{(B.11)}$$

Let us remark that for any scalar function U:

$$U \operatorname{div}\{\boldsymbol{\xi}_1 \operatorname{div}\boldsymbol{\xi}_1 - \nabla\boldsymbol{\xi}_1(\boldsymbol{\xi}_1)\} + \nabla\nabla(U)\boldsymbol{\xi}_1\cdot\boldsymbol{\xi}_1 + 2f\operatorname{grad} U\cdot\boldsymbol{\xi}_1 \operatorname{div}\boldsymbol{\xi}_1 = \operatorname{div}\{U\boldsymbol{\xi}_1 \operatorname{div}\boldsymbol{\xi}_1 - U\nabla\boldsymbol{\xi}_1(\boldsymbol{\xi}_1) + \operatorname{grad} U\cdot\boldsymbol{\xi}_1\boldsymbol{\xi}_1\}. \qquad \text{(B.12)}$$

Setting $U = r^k$ in that relation and substituting it into (B.11) yield (B.4). Expressing the three last terms of (B.4) in spherical coordinates gives (B.5).

Taking fY_ℓ^m instead of f, assuming that $\boldsymbol{\xi}_1$ and $\boldsymbol{\xi}_2$ are radial, and noting that $\delta_{1e} Y_\ell^m = 0$, $\delta_{1l} Y_\ell^m = 0$, and $\delta_{2l} Y_\ell^m = 0$, relations (B.2), (B.3), and (B.5) give the perturbations of $\mathcal{F} = \int_V f(x) r^k Y_\ell^m \,\mathrm{d}V$:

$$\delta_1\mathcal{F} = \int_{V_0} r^k \delta_{1e} f Y_\ell^m \,\mathrm{d}V - \int_{\Sigma_0} r^k [f\boldsymbol{\xi}_1\cdot\boldsymbol{n}] Y_\ell^m \,\mathrm{d}\Sigma, \qquad \text{(B.13)}$$

$$\delta_1\mathcal{F} = \int_{V_0} (r^k \delta_{1l} f + f\operatorname{div}(r^k\boldsymbol{\xi}_1)) Y_\ell^m \,\mathrm{d}V, \qquad \text{(B.14)}$$

$$\delta_2\mathcal{F} = \int_{V_0} \{r^k \delta_{2l} f + 2\delta_{\mathrm{l}} f \operatorname{div}(r^k \boldsymbol{\xi}_1) + f(\operatorname{div}(r^k \boldsymbol{\xi}_2) + (k+2)) f \operatorname{div}(\xi_1^2 r^{k-1}\boldsymbol{e}_\mathrm{r})\} Y_\ell^m \,\mathrm{d}V. \qquad \text{(B.15)}$$

It yields

$$\delta\mathcal{F} = \int_{V_0} (r^k \delta_{\mathrm{l}} f + f\operatorname{div}(r^k\boldsymbol{\xi})) Y_\ell^m \,\mathrm{d}V + \int_{V_0} (\delta_{1l} f \operatorname{div}(r^k\boldsymbol{\xi}) + (k+2) f \operatorname{div}(\xi^2\, r^{k-1}\boldsymbol{e}_\mathrm{r})/2) Y_\ell^m \,\mathrm{d}V, \qquad \text{(B.16)}$$

with (see (19)–(21))

$$\delta\mathcal{F}_\ell^m = \delta_1\mathcal{F} + \frac{1}{2}\delta_2\mathcal{F}, \qquad \boldsymbol{\xi} = \boldsymbol{\xi}_1 + \frac{1}{2}\boldsymbol{\xi}_2,$$

$$\delta_{\mathrm{l}} f = \delta_{1l} f + \frac{1}{2}\delta_{2l} f. \qquad \text{(B.17)}$$

Eq. (B.16) yields (37) by taking $k = \ell$ and $f = \rho$, i.e. $\mathcal{F} = \phi_\ell^m$.

Note that taking $k = 2$ and $Y_\ell^m = Y_0^0 = 1$ corresponds to the perturbation of inertia considered in Chambat and Valette (2001).

Appendix C. Expression of C_ℓ^m

Let us define the functions X_ℓ of (θ, λ) as

$$X_\ell = \int_0^b \delta_{\rm d}\rho\, r^{\ell+2}\,{\rm d}r - \sum_{r_\Sigma}[\rho]\xi_{\rm d} r_\Sigma^{\ell+2}. \tag{C.1}$$

We aim to express (see Eq. (69))

$$C_\ell^m = -\frac{2}{3\sqrt{5}}\epsilon(b)(\ell+3)\int_\Omega X_\ell Y_2^0 Y_\ell^m\,{\rm d}\Omega \tag{C.2}$$

as a function of (see Eq. (46))

$$L_\ell^m = \int_\Omega X_\ell Y_\ell^m\,{\rm d}\Omega. \tag{C.3}$$

For that purpose, we use the expansion

$$Y_2^0 Y_\ell^m = \sum_{\ell' m'} \gamma_{\ell\,\ell'\,2}^{m\,m'\,0} Y_{\ell'}^{m'}, \tag{C.4}$$

that yields, for any function h

$$\int_\Omega h Y_2^0 Y_\ell^m\,{\rm d}\Omega = 4\pi \sum_{\ell' m'} \gamma_{\ell\,\ell'\,2}^{m\,m'\,0} h_{\ell'}^{m'}, \tag{C.5}$$

where the γ are defined in a similar way as for the complex spherical harmonics (e.g. Dahlen, 1976; Balmino, 1994) by

$$\gamma_{\ell\,\ell'\,s}^{m\,m'\,t} = \frac{1}{4\pi}\int_\Omega Y_{\ell'}^{m'} Y_\ell^m Y_s^t\,{\rm d}\Omega. \tag{C.6}$$

For $(s, t) = (2, 0)$, they are related to the Wigner 3-j symbols (see e.g. Weisstein (2004) or Rotenberg et al., 1959) by

$$\gamma_{\ell\,\ell'\,2}^{m\,m'\,0} = (-1)^m\sqrt{5(2\ell+1)(2\ell'+1)}\begin{pmatrix}\ell & \ell' & 2\\ 0 & 0 & 0\end{pmatrix} \times \begin{pmatrix}\ell & \ell' & 2\\ -m & m' & 0\end{pmatrix}.$$

The selection rules of the Wigner 3-j symbols imply that $\gamma_{\ell\,\ell'\,2}^{m\,m'\,0}$ is null unless $m = m'$, and $\ell' = \ell - 2, \ell, \ell+2$ for $\ell \geq 2$ or $\ell' = 1, 3$ for $\ell = 1$. Thus, the expansion (C.4) can then be simplified in

$$Y_2^0 Y_\ell^m = \gamma_{\ell\,\ell-2\,2}^{m\,m\,0} Y_{\ell-2}^m + \gamma_{\ell\,\ell\,2}^{m\,m\,0} Y_\ell^m + \gamma_{\ell\,\ell+2\,2}^{m\,m\,0} Y_{\ell+2}^m, \tag{C.7}$$

where the first term of the right-hand side is implicitly null for $|m| > \ell - 2$. These γ can be evaluated with the expressions given, e.g. by Landau and Lifchitz (1967, p. 106):

$$\gamma_{\ell\,\ell\,2}^{m\,m\,0} = \sqrt{5}\frac{\ell(\ell+1) - 3m^2}{(2\ell-1)(2\ell+3)}, \tag{C.8}$$

$$\gamma_{\ell\,\ell-2\,2}^{m\,m\,0} = \frac{3}{2}\sqrt{5}\left(\frac{((\ell-1)^2 - m^2)(\ell^2 - m^2)}{(2\ell-3)(2\ell-1)^2(2\ell+1)}\right)^{1/2}, \tag{C.9}$$

$$\gamma_{\ell\,\ell+2\,2}^{m\,m\,0} = \frac{3}{2}\sqrt{5}\left(\frac{((\ell+1)^2 - m^2)((\ell+2)^2 - m^2)}{(2\ell+1)(2\ell+3)^2(2\ell+5)}\right)^{1/2}. \tag{C.10}$$

By substituting (C.7) into (C.2), C_ℓ^m can be rewritten as

$$C_\ell^m = -\frac{2}{3\sqrt{5}}\epsilon(b)(\ell+3)\left\{\gamma_{\ell\,\ell-2\,2}^{m\,m\,0}\int_\Omega X_\ell Y_{\ell-2}^m\,{\rm d}\Omega + \gamma_{\ell\,\ell\,2}^{m\,m\,0}\int_\Omega X_\ell Y_\ell^m\,{\rm d}\Omega + \gamma_{\ell\,\ell+2\,2}^{m\,m\,0}\int_\Omega X_\ell Y_{\ell+2}^m\,{\rm d}\Omega\right\}. \tag{C.11}$$

Supposing that the non-hydrostatic variations lie in the uppermost part of the Earth, we use the approximation $r^{\ell+2} \simeq r^\ell b^2$ (or $r^{\ell-2} \simeq r^\ell/b^2$) to deduce that $X_\ell \simeq b^2 X_{\ell-2}$ and $X_\ell \simeq b^{-2} X_{\ell+2}$, and thus

$$C_\ell^m = -\frac{2}{3\sqrt{5}}\epsilon(b)(\ell+3)\left\{\gamma_{\ell\,\ell-2\,2}^{m\,m\,0} b^2 L_{\ell-2}^m + \gamma_{\ell\,\ell\,2}^{m\,m\,0} L_\ell^m + \gamma_{\ell\,\ell+2\,2}^{m\,m\,0} b^{-2} L_{\ell+2}^m\right\}. \tag{C.12}$$

Let $\delta_{\rm d} g$ and $\zeta_{\rm d}$ be the linear deviatoric gravity and height anomaly corresponding to L_ℓ^m. These two quantities are related to L_ℓ^m by a relation similar to (10):

$$L_\ell^m = \frac{4\pi\rho_2}{3}b^{\ell+3}\left(2\frac{\delta_{\rm d} g_\ell^m}{g} + 3\frac{\zeta_{{\rm d}\,\ell}^m}{b}\right) = \frac{4\pi\rho_2}{3}b^{\ell+3} Z_\ell^m, \tag{C.13}$$

with

$$Z = 2\frac{\delta_{\rm d} g}{g} + 3\frac{\zeta_{\rm d}}{b}. \tag{C.14}$$

Substituting (C.13) into (C.12) yields

$$C_\ell^m = -\frac{8\pi\rho_2}{9\sqrt{5}}\epsilon(b)(\ell+3)b^{\ell+3}(\gamma_{\ell\,\ell-2\,2}^{m\,m\,0}Z_{\ell-2}^m + \gamma_{\ell\,\ell\,2}^{m\,m\,0}Z_\ell^m + \gamma_{\ell\,\ell+2\,2}^{m\,m\,0}Z_{\ell+2}^m). \tag{C.15}$$

The corresponding height anomaly is

$$\zeta_{C\ell}^m = -\frac{2\epsilon(b)}{3\sqrt{5}}\frac{\ell+3}{2\ell+1}b(\gamma_{\ell\,\ell-2\,2}^{m\,m\,0}Z_{\ell-2}^m + \gamma_{\ell\,\ell\,2}^{m\,m\,0}Z_\ell^m + \gamma_{\ell\,\ell+2\,2}^{m\,m\,0}Z_{\ell+2}^m). \tag{C.16}$$

This is the most suitable formula in order to numerically evaluate ζ_C in function of Z. It also yields, with the help of (C.5)

$$\zeta_{C\ell}^m = -\frac{\epsilon(b)}{6\pi\sqrt{5}}\frac{\ell+3}{2\ell+1}b\int_\Omega ZY_2^0 Y_\ell^m \,\mathrm{d}\Omega, \tag{C.17}$$

that is (70).

References

Balmino, G., Lambeck, K., Kaula, W., 1973. Spherical harmonic analysis of the Earth's topography. J. Geophys. Res. 78 (2), 478–481.

Balmino, G., 1994. Gravitational potential harmonics from the shape of an homogeneous body. Celestial Mech. Dyn. Astron. 60, 331–364.

Belleguic, V., 2004. Étude de la lithosphère et des volcans martiens à partir des données de gravité et de topographie, Thése de Doctorat, IPG Paris.

Chambat, F., Valette, B., 2001. Mean radius, mass and inertia for reference Earth's models. Phys. Earth Planet. Int. 124, 237–253.

Dahlen, F.A., 1976. The passive influence of the oceans upon the rotation of the Earth. Geophys. J. R. Astron. Soc. 46, 363–406.

Denis, C., 1989. The hydrostatic figure of the Earth. In: Teisseyre, R. (Ed.), Gravity and Low Frequency Geodynamics. Physics and Evolution of the Earth's Interior, vol. 4. Elsevier (chapter 3).

Hager, B.H., Clayton, R.W., 1989. Constraints on the structure of mantle convection using seismic observation, flow models and the geoid. In: Peltier, W.R. (Ed.), Mantle Convection, Plate Tectonics and Global Dynamics. Gordon and Breach Science Publishers, New York.

Heiskanen, W.A., Moritz, H., 1967. Physical Geodesy. W.H. Freeman and Company.

Ilk, K.H., Ricard, Y., Rummel, R., Thalhammer, M., 1996. Application of spaceborne gravimetry to research on the interior of the Earth. In: Study of advanced reduction methods for spaceborne gravimetry data, and of data combination with geophysical parameters, CIGAR IV Midterm Report, Pub. H. Sünkel, Graz.

Ishii, M., Tromp, J., 2001. Even-degree lateral variations in the Earth's mantle constrained by free oscillations and the free-air gravity anomaly. Geophys. J. Int. 145, 77–96.

Kaban, M.K., Schwintzer, P., Tikhotsky, S.A., 1999. A global isostatic gravity model of the Earth. Geophys. J. Int. 136, 519–536.

Landau, L., Lifchitz, E., 1967. Mécanique quantique, Théorie non relativiste. 3e édition, Ed. Mir, Moscou.

Lemoine et al., 1998. The development of the joint NASA GSFC and the National Imagery and Mapping Agency (MIMA) Geopotential Model EGM96. NASA Technical Paper, ref. NASA/TP-1998–206861, NASA Goddard Space Flight Center, Greenbelt, Maryland.

Martinec, Z., 1994. The density contrast at the Mohorovicic discontinuity. Geophys. J. Int. 117, 539–544.

Moritz, H., 1990. The Figure of the Earth. Wichmann.

Nahavandchi, H., Sjöberg, L.E., 1998. Terrain corrections to power H^3 in gravimetric geoid determination. J. Geodesy 72, 124–135.

Ockendon, J.R., Turcotte, D.L., 1977. On the gravitational potential and field anomalies due to thin mass layers. Geophys. J. R. Astron. Soc. 48, 479–492.

Oldenburg, D.W., 1974. The inversion and interpretation of gravity anomalies. Geophysics 39 (4), 526–536.

Parker, R.L., Huestis, S.P., 1974. The inversion of magnetic anomalies in the presence of topography. J. Geophys. Res. 79 (11), 1587–1593.

Rapp, R.H., 1997. Use of potential coefficient models for geoid undulation determinations using a spherical harmonic representation of the height anomaly/geoid undulation difference. J. Geodesy 71, 282–289.

Ricard, Y., Vigny, C., 1989. Mantle dynamics with induced plate tectonics. J. Geophys. Res. 94 (B12), 17543–17559.

Rotenberg, M., Bivens, R., Metropolis, N., Wooten, J.K., 1959. The 3*j* and 6*j* Symbols. MIT Press, Cambridge, MA.

Sjöberg, L.E., 1995. On the quasigeoid to geoid separation. Manuscripta Geodetica 20, 182–192.

Sjöberg, L.E., 1998a. On the Pratt and Airy models of isostatic geoid undulations. J. Geodynamics 26 (1), 137–147.

Sjöberg, L.E., 1998b. The exterior Airy/Heiskanen topographic-isostatic gravity potential, anomaly and the effect of analytical continuation in Stokes' formula. J. Geodesy 72, 654–662.

Zharkov, V.N., Trubitsyn, V.P., Hubbard, W.B. (Ed.), 1978. Physics of Planetary Interiors. Pachart Pub. House, Tucson, Ariz, p. 388

Weisstein, E.W. Wigner 3*j*-Symbol, from MathWorld—A Wolfram Web Resource, http://mathworld.wolfram.com/Wigner3j-Symbol.html.